Service Velocity: Rapid Provisioning Strategies in Optical ROADM Networks

Sheryl L. Woodward, Mark D. Feuer, Inwoong Kim, Paparao Palacharla, Xi Wang, and Daniel Bihon

***Abstract*—The advent of reconfigurable optical add/drop multiplexers with colorless and non-directional add/drop ports enables transponders and regenerators to be pre-deployed, without *a priori* knowledge of which wavelength or direction they will eventually serve. We study pre-deployment of optical regenerators as a means to drastically reduce the provisioning time, using Monte Carlo simulation of an optical backbone network. With appropriate placement strategies, regenerators can be efficiently pre-deployed so that new connections can be established rapidly, without the delays caused by service visits to intermediate network nodes.**

***Index Terms*—Optical fiber communication; Optical fiber networks; ROADM; Wavelength-routed networks.**

I. Introduction

The introduction of reconfigurable optical add/drop multiplexers (ROADMs) in optical communication networks has already significantly lowered costs and dramatically simplified operations, thanks to the ability to remotely reconfigure an optical bypass for specific wavelength channels across the network [1]. The latest generation of ROADMs continues these trends toward increased efficiency by including colorless non-directional (CN) add/drop ports, so that any transponder or regenerator can serve any wavelength channel on any fiber route. This added flexibility to reconfigure the network remotely, without manual intervention, is known to be valuable in a wide variety of applications [1–9]. CN ROADMs are especially essential for dynamic networking because they enable the efficient sharing of transponders [2]. Others have already described how such ROADMs will enable shared mesh restoration [3] and wavelength grooming (also referred to as network defragmentation) [4]. Bridge and roll functionality, a necessary component for wavelength grooming and many other maintenance functions, has already been experimentally demonstrated in the laboratory [5].

For networks to achieve fully dynamic operation, not only technology, but also business models and network operations must evolve. While the CN ROADM technology is clearly a crucial technological advance in this direction, a key application driver for CN ROADMs may be the ability to pre-deploy regenerators in support of accelerated connection provisioning in the network [6,7]. If all needed regenerators are pre-deployed, a new circuit can be remotely provisioned without requiring manual operations at any intermediate nodes, enabling new connections to become operational with minimal delay.

We refer to this concept as *service velocity*, and it is the focus of this work. In a network supporting service velocity, when a customer requests a connection between Los Angeles and New York, as soon as their equipment is connected at the end locations, the connection can be completed using regenerators already in place in the network. Not only does the service velocity concept dramatically reduce the time it takes to provision new circuits, it also enables $1:N$ sparing of regenerators. If any regenerator fails, another path can be remotely established using pre-deployed regenerators to restore service. While this concept does not require a dramatic new business model, and is only an incremental change in standard operating procedures, it is one step on the path from a quasi-static to a dynamic network.

Here, we introduce several regenerator placement strategies that ensure service velocity and compare their efficiency and effectiveness using network simulations realized by Monte Carlo methods. Network cost is characterized in terms of the number of deployed regenerators and the number of truck rolls needed to place them, tabulated over time as the network traffic grows. Unlike previous studies [10], our work takes into account intra-node contention that may occur within the CN ROADM. (Contention-free CN ROADMs are not currently being deployed, as technologies for a practical and scalable architecture are not yet feasible. At this time, it is far more cost effective to manage the intra-node contention than to build a truly contention-free CN ROADM [11–13]).

The rest of this paper is organized as follows. In Section II, we discuss the network topology, traffic patterns, and mode of operation; Section III describes the service velocity algorithms; and in Section IV, details of the simulations are presented. In Sections V and VI, results are presented and discussed.

II. Network Model

Most of the network parameters used for our study reflect operating realities for a continental-scale backbone network in the near-term future, although some additional assumptions were made to simplify the problem.

Manuscript received August 12, 2011; revised December 15, 2011; accepted December 15, 2011; published January 16, 2012 (Doc. ID 152793).

Sheryl L. Woodward (e-mail: sheri@research.att.com) and Mark D. Feuer are with AT&T Optical Systems Research, Middletown, New Jersey 07733, USA.

Inwoong Kim, Paparao Palacharla, and Xi Wang are with Fujitsu Laboratories of America, Richardson, Texas 75082, USA.

Daniel Bihon is with Fujitsu Network Communications, Richardson, Texas 75082, USA.

Digital Object Identifier 10.1364/JOCN.4.000092

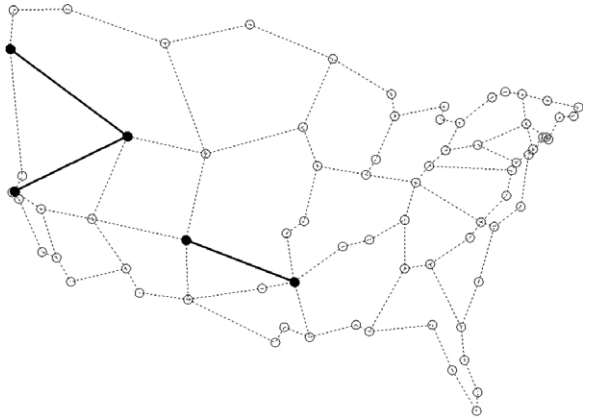

Fig. 1. The network topology is a modified version of the DARPA CORONET topology for the Contiguous United States [15]. This topology has 75 nodes and 99 links; the link distance of the three links shown as solid lines was truncated to 1000 km so that simulations could be performed with an optical reach of 1000 km. The original distance of all three of these links was below 1225 km.

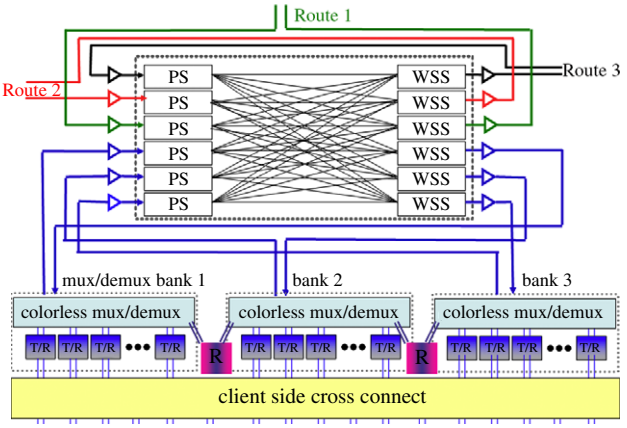

Fig. 2. (Color online) The ROADM architecture uses a broadcast and select core and is both colorless and non-directional [8,9]. Because of wavelength contention on the connection between the colorless mux/demux and the ROADM core, to support same-wavelength regeneration, each regenerator must connect to two different mux/demux banks, effectively grouping regenerators into $B(B-1)/2$ regenerator sets.

First, we assume that traffic is quasi-static: it grows over time in a random fashion, yet, once a circuit is established, it persists indefinitely. This is substantially true today, and will likely remain so for some time as networks slowly evolve toward fully dynamic operation. Two different traffic models are studied: uniform traffic, in which all source–destination pairs are equiprobable; and population-based traffic, in which the probability of traffic terminating at a node is proportional to the population of the surrounding area [14]. In census areas that include multiple nodes (New York, Miami, and Philadelphia) the population of the metropolitan area is divided equally between the nodes. Note that this is an imperfect proxy for traffic, as it does not account for business centers or for the population residing outside of these metropolitan areas. However, it is straightforward to replicate and is more representative of real traffic than a uniform traffic matrix.

Our network topology was based on that of the DARPA CORONET (Core Optical Networks) program, selecting only the Contiguous United States nodes (see Fig. 1) [15]. This publicly available topology is a realistic approximation of a continental-scale core network. We truncated the distance on the three longest links of the CORONET topology to 1000 km, so that we could directly compare simulation results obtained with 1000 and 2000 km optical reach values. In a real network, Raman amplification could be used to cost-effectively extend the reach on these few links, if desired. We also assumed that the entire network topology (nodes and their interconnections) is present when we first begin adding traffic to the network.

To reflect the growth of the network over time, we augmented capacity on a link-by-link basis by adding additional fiber pairs as traffic between two nodes threatened to exhaust a link's capacity (e.g., exceeded a wavelength usage threshold). This augmentation process, uncommon in network simulations, is important for three reasons. First, it reflects major carriers' actual practice, attempting to forecast route exhaust and activate additional line systems in anticipation of traffic growth. Second, we found that, when we simply discarded blocked demands (a common simulation practice), then the traffic matrix quickly became distorted from its original distribution. Third, as-needed augmentation is in keeping with the service velocity concept—that resources are deployed just in time, to minimize capital expenditures while serving all demands without delay.

We assumed that the transmission equipment supported 88 wavelengths per fiber and that the optical reach was either 1000 km or 2000 km.

The ROADM architecture depicted in Fig. 2 was used. This is a colorless non-directional ROADM architecture, in which any transponder can provide any wavelength to any inter-node fiber pair. There is some possibility of contention, as each mux/demux bank can only service a single copy of any given wavelength to the network. We have previously shown that this contention is quite manageable in fully dynamic networks without dedicated regenerators, as long as the number of mux/demux banks (these are also referred to as transponder banks [9]) equals the number of inter-node fiber pairs [12]. In the present simulations, the number of mux/demux banks B was kept equal to the number of inter-node fiber pairs served, which means that any add/drop fraction up to 100% is possible. The ROADM of Fig. 2 can grow while in service, so, as a link's capacity was augmented by lighting another fiber pair, additional mux/demux banks were added to each of the ROADMs serving the link. The simulations were capped at a maximum of three fiber pairs per inter-node link.

To permit regeneration without wavelength change, each regenerator needs to connect to two banks. With B mux/demux banks, this means that each node has $B(B-1)/2$ regenerator sets. We assumed that existing connections would not be required to change wavelength when a new connection is added, so regenerators in some sets may be unable to access certain wavelengths at certain times.

We also preserved the current operating preference for wavelength continuity (i.e., no recoloring) at regenerator sites.

Historically, this has been done to simplify maintenance procedures, a justification that might not persist as manual procedures are replaced with greater automation. We explored the effect of allowing regenerators to recolor circuits at regeneration points, but did not see any significant change in performance. The results presented in this paper are achieved without any recoloring.

III. Service Velocity Algorithms

The primary focus of our study is the pre-deployment of regenerators in support of service velocity (SV). The ideal pre-deployment strategy should provide enough resources to guarantee SV for every new demand while minimizing the capital expense represented by idle regenerators (i.e., those deployed but not in use). At the same time, capital expense must be balanced against the operating expense of "truck rolls" in which new regenerators are deployed. Meeting these objectives is the job of the SV algorithm. Each time a node puts a pre-deployed regenerator into service, the SV algorithm is run to see if more regenerators are needed to meet future demands. If so, the algorithm determines how many to deploy at each node and in which regenerator sets to install them.

In our simulations, we compared three SV algorithms. The first algorithm is referred to as the Simple SV (SSV). This algorithm is local to each node, requiring no knowledge of remote resources or network state. First, the SSV inventories the available wavelengths on each inter-node fiber pair (degree) and on each regenerator set (recall that each mux/demux bank can only serve a single copy of a given wavelength). If there is any pair of available wavelengths on any pair of degrees that cannot be served by an existing idle regenerator, then a truck roll is initiated, and enough regenerators are added to "unblock" all of the available wavelength–degree pairs at that node. To reduce truck rolls, a minimum of R_{add} regenerators is pre-deployed per truck roll (in our tests $R_{\text{add}} = 2$ or 4) and these are placed in the regenerator sets that can serve the largest number of wavelengths.

The second algorithm tested is referred to as local constraint-aware service velocity (LC-SV). This algorithm is also local to each node. However, instead of adding regenerators to ensure connectivity between *all* available wavelength–degree pairs, the LC-SV variant adds regenerators only when needed to ensure *at least one* common wavelength between each degree pair. This reduces the number of idle regenerators as well as truck rolls compared to the SSV case, but there is a slight possibility of service velocity failure if the supported wavelengths within the node do not align with the available wavelengths along the circuit's entire path.

Finally, we simulated a more complex algorithm: global constraint-aware SV (GC-SV). In this option, knowledge of path routing and network state is used to verify that at least one common wavelength exists for each possible *path* going through a node. GC-SV eliminates the blocking present in LC-SV, yet is more efficient than SSV. Due to its dependence on path routing information, GC-SV may be most suitable when the number of allowed paths from source A to destination Z is limited.

IV. Simulation Method

We used Monte Carlo simulations to calculate the number of regenerators deployed over time in a large backbone network (shown in Fig. 1) implementing the SV concept. As noted above, this is a quasi-static scenario in which connections are randomly generated one at a time and persist indefinitely. The endpoints are chosen randomly, with either uniform probability or with a population-weighted probability. All connections were at the same rate (e.g., 100 Gbps).

Shortest path routing was used, and the regenerator location(s) along each path were pre-determined. For each path, the number of regenerators used was based on optical reach considerations only (e.g., no additional regenerators for reducing network blocking via wavelength recoloring) and regenerator locations were set by allowing each lightpath to travel as far as possible before being regenerated. The wavelength assignment algorithm took into account any intra-node wavelength contention [13].

At the beginning of the simulation, each possible regenerator location had R_{ini} regenerators pre-deployed, and the minimum number of regenerators added in a truck roll was R_{add}.

In tests without dynamic link augmentation, only approximately 300 demands could be served before network blocking appeared (network blocking denotes the lack of a continuous wavelength along the needed fiber segments, assuming no limitation due to node equipment). When the number of inter-node fiber pairs was tripled on all links, then almost 1000 demands could be served before network congestion blocked service. Therefore, we explored dynamic link augmentation with a maximum augmentation of three fibers per link. Utilizing thresholds of 80%, 70%, and 60% wavelength usage, network blocking appeared at approximately 400, 500, and 1000 demands, respectively. Changing the augmentation threshold had no significant affect on the number of regenerators used (at 300 demands it varied by no more than 0.1%).

The blocking performance of the network with dynamic link augmentation utilizing a threshold of 60% wavelength usage was comparable to that of a network with three fiber pairs per link, even though very few links reached the maximum upgrade of three fiber pairs. In additional simulations employing k-shortest path routing, we found that, with a 60% threshold for augmenting a link's capacity, the shortest path was always utilized when the network was in the zero-blocking regime.

After each connection was provisioned, an SV algorithm was run (either SSV, LC-SV, or GC-SV) to determine the truck rolls and regenerators needed.

Simulations were performed for a variety of cases:

- $(R_{\text{ini}}, R_{\text{add}}) = (1, 2)$ or $(2, 4)$
- Optical reach = 1000 km or 2000 km
- SV algorithm = SSV, LC-SV, or GC-SV
- Traffic density matrix = uniform or population-weighted

Additional simulations were performed assuming that a colorless, non-directional, contention-free (CNC) ROADM was used so that our results could be compared to an idealized case.

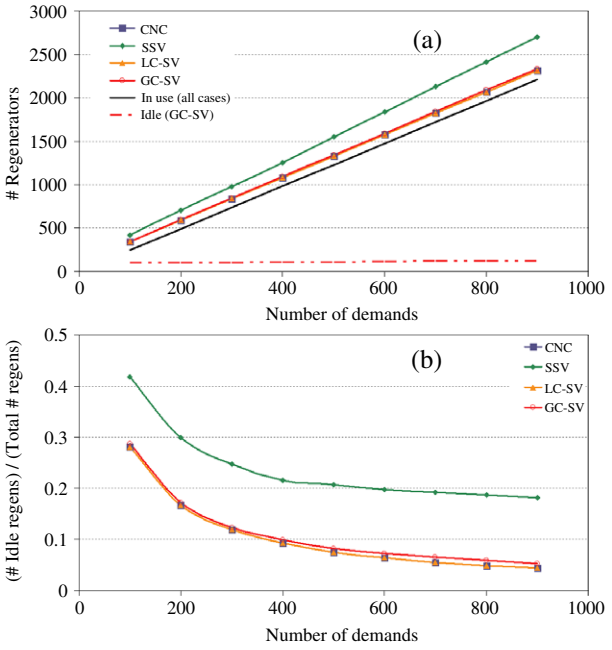

Fig. 3. (Color online) The regenerator usage for the case with a uniform traffic model, an optical reach of 1000 km, and $(R_{\text{ini}}, R_{\text{add}}) = (1, 2)$. The curves only cover the zero-blocking regime and stop at 900 connection requests. (a) Regenerator usage for various service velocity algorithms. The number of regenerators in use is the same for all cases. For comparison, results with an idealized CNC ROADM are also included. (b) The ratio of the number of idle regenerators over the total number of regenerators.

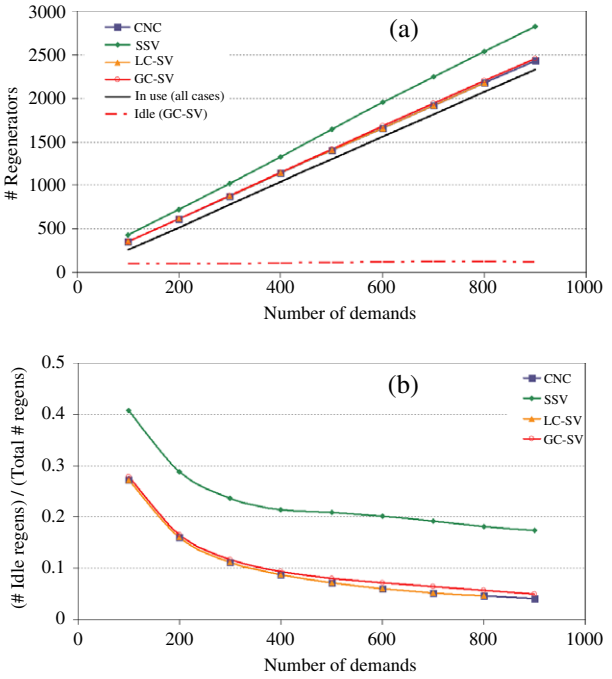

Fig. 4. (Color online) The regenerator usage for the case with a population-based traffic model, an optical reach of 1000 km, and $(R_{\text{ini}}, R_{\text{add}}) = (1, 2)$. As in Fig. 3, the curves only cover the zero-blocking regime. (a) Regenerator usage for various service velocity algorithms. (b) The ratio of the number of idle regenerators over the total number of regenerators.

Simulations were performed over 100 runs of 2000 demands, and averaged results are presented. In these simulations, the threshold for dynamic link augmentation was set to 60% wavelength usage. The simulation reported the number of regenerators installed in the network, and the number of those in service. It also counted the number of truck rolls (necessary to install regenerators). No results are presented for cases in which blocking occurs, since blocking is contrary to the service velocity concept and distorts the intended traffic pattern. Therefore, the result curves are truncated at ~900 demands.

V. Results

Figure 3(a) presents the number of regenerators deployed versus demand count for all three SV algorithms, with a 1000 km optical reach, $(R_{\text{ini}}, R_{\text{add}}) = (1, 2)$, and a uniform traffic density matrix. In addition, the results for an idealized CNC ROADM are also shown (without contention, the SSV, LC-SV, and GC-SV algorithms are equivalent). The number of regenerators in use is shown as a dashed line and is the same in all cases. Finally, the number of idle regenerators for the GC-SV case is shown (it is nearly identical for the LC-SV and CNC cases). For the SSV case, the number of idle regenerators is larger and increases with number of demands.

At 1000 demands there was some blocking; hence the curves are truncated at 900 demands. Blocking can occur either because of network congestion or because no regenerator at the pre-selected regenerator location is available that can provide the desired wavelength. For both the SSV and GC-SV algorithms, network congestion was the only cause of blocking at 1000 demands, while for the LC-SV there was also a small contribution due to regenerator blocking.

Figure 3(b) presents the data in a more normalized fashion: the number of idle regenerators divided by the total number of regenerators deployed, versus the number of demands.

Figures 4(a) and 4(b) present similar results for the case with a population-weighted traffic density matrix. In this case the curves for the LC-SV case are truncated at 800 demands, as a small amount of regenerator blocking occurred once 900 demands were reached (in the 100 simulation runs a total of 20 connection requests were blocked, for a blocking rate of 2×10^{-4}). Although more regenerators are required in the population-weighted case (probably due to a larger number of bi-coastal connection requests), the trends observed in the uniform traffic case hold true for this demand set as well.

Figures 5(a) and 5(b) compare regenerator counts obtained with $(R_{\text{ini}}, R_{\text{add}}) = (1, 2)$ to those found with $(R_{\text{ini}}, R_{\text{add}}) = (2, 4)$. A 1000 km optical reach was used, and a population-weighted demand set. By doubling $(R_{\text{ini}}, R_{\text{add}})$, the number of idle regenerators increases by 46%–68%, so that the utilization of regenerator resources is significantly reduced. Values vary for the different cases, but, for the GC-SV algorithm, the use of $(R_{\text{ini}}, R_{\text{add}}) = (2, 4)$ implies a nearly constant increase of 60 idle regenerators, compared to $(R_{\text{ini}}, R_{\text{add}}) = (1, 2)$. The capital expense of more regenerators must be balanced

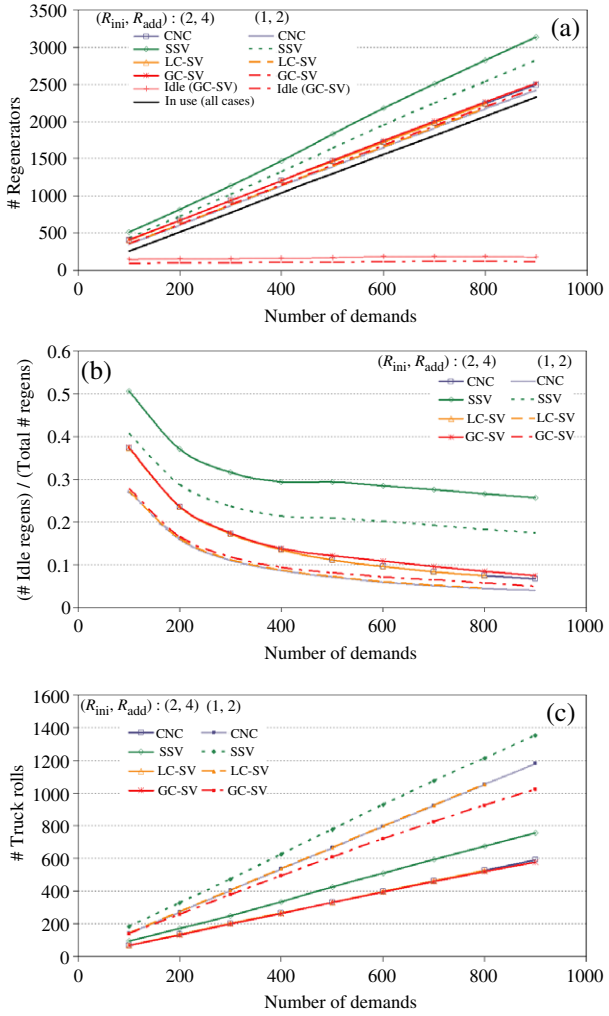

Fig. 5. (Color online) The effect on regenerator usage when the minimum number of regenerators deployed per truck roll is doubled (solid curves: $(R_{\text{ini}}, R_{\text{add}}) = (2, 4)$; dashed lines: $(R_{\text{ini}}, R_{\text{add}}) = (1, 2)$). The dashed lines are identical to the data presented in Fig. 4. Both cases used a population-based traffic model and an optical reach of 1000 km. (a) Regenerator usage for various service velocity algorithms. (b) The ratio of the number of idle regenerators over the total number of regenerators. (c) The number of truck rolls.

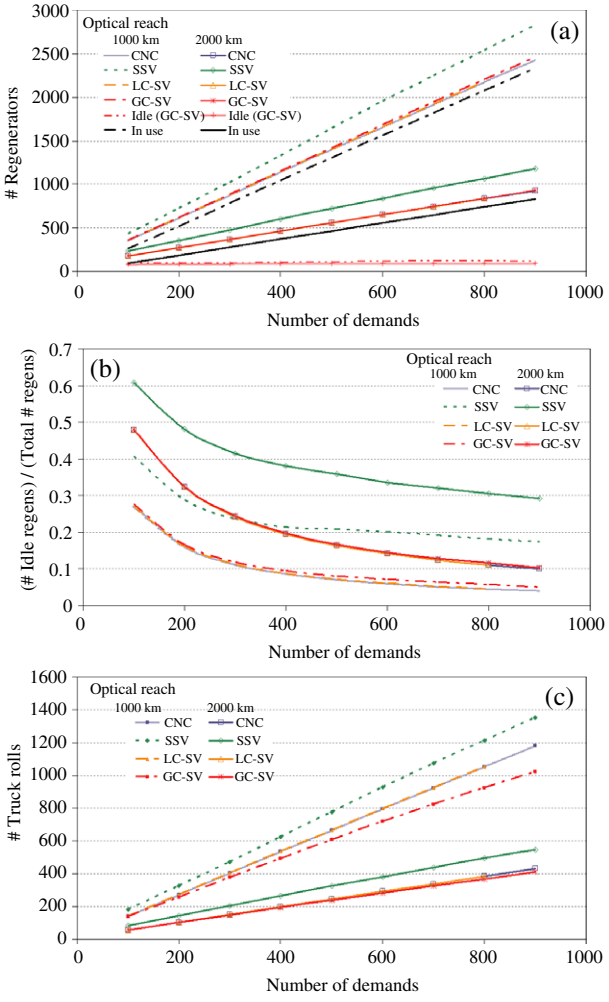

Fig. 6. (Color online) Regenerator usage for the case with a population-based traffic model, an optical reach of 2000 km, and $(R_{\text{ini}}, R_{\text{add}}) = (1, 2)$. For comparison, data shown in Fig. 4 with an optical reach of 1000 km is included as dashed lines. (a) Regenerator usage for various service velocity algorithms. (b) The ratio of the number of idle regenerators over the total number of regenerators. (c) The number of truck rolls.

against the operational savings of reduced truck rolls, which are shown in Fig. 5(c). When $(R_{\text{ini}}, R_{\text{add}})$ is doubled, the number of truck rolls is decreased by 40%–50%. A full economic analysis of this tradeoff is beyond the scope of this paper and would be dependent on the details of each network studied. It is interesting to note that the GC-SV algorithm achieves significantly lower truck rolls than the other algorithms, for the same number of deployed regenerators. Apparently, GC-SV is more effective in grouping its regenerator installs into less frequent service visits, especially for the $(R_{\text{ini}}, R_{\text{add}}) = (1, 2)$ case.

Figure 6 compares the results obtained with a 1000 km optical reach with those obtained with a 2000 km optical reach. The population-weighted demand set was used, and $(R_{\text{ini}}, R_{\text{add}}) = (1, 2)$. While the trends in the two data sets are comparable, this clearly shows the advantages of increasing the optical reach. Not only is the number of working regenerators required in the 2000 km optical reach case significantly reduced, but the number of idle regenerators is also lower, as fewer nodes are used for optical regeneration (for the 1000 km reach case, 68 nodes contained regenerators, while, for the 2000 km reach case, 64 nodes contained regenerators; no intentional effort was made to consolidate the set of nodes used for regeneration).

VI. Discussion and Future Work

We explored three different strategies for pre-deployment of regenerators, all designed to support the SV concept. Because no knowledge of path routing or network state was utilized, SSV was the least efficient of the three algorithms studied; it required more regenerators to be pre-deployed and more truck

rolls than the other algorithms. While network blocking was always the dominant component for SSV and GC-SV, a small amount of regenerator blocking could occur with the LC-SV approach. Finally, GC-SV has slightly fewer truck rolls than the others, apparently because it tends to install more than the minimum number of regenerators per truck roll.

Based on the results presented here, we believe that pre-deployment of regenerators can be a cost-effective way to provide high-velocity wavelength services in next-generation networks of colorless non-directional ROADMs. Our simulations of quasi-static network traffic growth show that the total number of pre-deployed regenerators grows smoothly with demand, aligning with the pay-as-you-grow business model preferred by many network operators. The number of regenerators standing idle, waiting to be used, saturates quickly at a modest level, so that regenerator utilization well over 90% is achieved for an optical reach of 1000 km. Since these idle regenerators can also provide $1:N$ protection against failure of working regenerators, they eliminate the need to keep spares stockpiled at nodes or regional depots.

Confirming our earlier results with add/drop transponders, we find that wavelength contention within the CN ROADMs is insignificant, as long as (1) the number of mux/demux banks is equal to the number of inter-node fiber pairs and (2) the wavelength assignment and the service velocity algorithms are contention aware [12,13].

In this work, we have considered a service velocity model that guarantees rapid provisioning for only a single wavelength demand. Multiple simultaneous demands may be supported, depending on the details of the demands and the network state. SV guarantees for multiple simultaneous demands will require minor changes to the service velocity algorithm, and some increase in the idle regenerator count may be anticipated. One important example of simultaneous demands would be diverse routing for survivability.

In order to achieve further reductions in the number of idle regenerators, it may be desirable to concentrate all regeneration into a limited subset of network nodes. Previous studies on such concentration [10] have not considered ROADM contention, so it will be important to confirm that our successful service velocity algorithms remain effective with the reduced set of regeneration sites. Since any regenerator concentration scheme necessarily implies routing constraints, the diverse path routing mentioned above may present a special challenge for site concentration.

ACKNOWLEDGMENT

We gratefully acknowledge many useful conversations with and suggestions from Martin Birk, Kathy Tse, Weiyi Zhang, and Peter Magill.

REFERENCES

[1] M. D. Feuer, D. C. Kilper, and S. L. Woodward, "ROADMs and their system applications" in *Optical Fiber Telecommunications, Volume B: Systems and Networks*. Elsevier Inc., London, UK, 2008, and references therein.

[2] A. L. Chiu, G. Choudhury, G. Clapp, R. Doverspike, M. Feuer, J. W. Gannett, J. Jackel, G. T. Kim, J. G. Klincewicz, T. J. Kwon, G. Li, P. Magill, J. M. Simmons, R. A. Skoog, J. Strand, A. Von Lehmen, B. J. Wilson, S. L. Woodward, and D. Xu, "Architectures and protocols for capacity efficient, highly dynamic and highly resilient core networks," *J. Opt. Commun. Netw.*, vol. 4, pp. 1–14, Jan. 2012.

[3] J. Strand and A. Chiu, "Realizing the advantages of optical reconfigurability and restoration with integrated optical cross-connects," *J. Lightwave Technol.*, vol. 21, pp. 2871–2882, 2003.

[4] G. Wellbrock, "Preparing for the future," in *Proc. ECOC*, Torino, Italy, 2010, Th.9.G.1.

[5] X. J. Zhang, M. Birk, A. Chiu, R. Doverspike, M. D. Feuer, P. Magill, E. Mavrogiorgis, J. Pastor, S. L. Woodward, and J. Yates, "Bridge-and-roll demonstration in GRIPhoN (Globally Reconfigurable Intelligent Photonic Network)," in *Technical Digest of OFC/NFOEC 2010*, 22–25 Mar. 2010, NThA1.

[6] K. A. Tse and M. Birk, private communication.

[7] P. Roorda and B. Collings, "Evolution to colorless and directionless ROADM architectures," in *Technical Digest of OFC/NFOEC 2008*, San Diego, CA, 2008, NWE2.

[8] S. L. Woodward, M. D. Feuer, J. Calvitti, K. Falta, and J. M. Verdiell, "A high-degree photonic cross-connect for transparent networking, flexible provisioning & capacity growth," in *Proc. of the European Conf. on Optical Communications*, 2006, Th1.2.2.

[9] S. L. Woodward, M. D. Feuer, J. L. Jackel, and A. Agarwal, "Massively-scaleable highly-dynamic optical node design," in *Technical Digest of OFC/NFOEC 2010*, 22–25 Mar. 2010, JThA18.

[10] X. Yang and B. Ramamurthy, "Dynamic routing in translucent WDM optical networks," in *Proc. of IEEE ICC 2002*, New York, Apr. 2002, vol. 5, pp. 2796–2802.

[11] S. L. Woodward, M. D. Feuer, P. Palacharla, X. Wang, I. Kim, and D. Bihon, "Intra-node contention in a dynamic, colorless, non-directional ROADM," in *Technical Digest of OFC/NFOEC 2010*, 22–25 Mar. 2010, PDPC8.

[12] M. D. Feuer, S. L. Woodward, P. Palacharla, X. Wang, I. Kim, and D. Bihon, "Intra-node contention in dynamic photonic networks," *J. Lightwave Technol.*, vol. 29, pp. 529–535, 2011.

[13] P. Palacharla, X. Wang, I. Kim, D. Bihon, M. D. Feuer, and S. L. Woodward, "Blocking performance in dynamic optical networks based on colorless, non-directional ROADMs," in *Technical Digest of OFC/NFOEC 2011*, 6–10 Mar. 2011, JWA8.

[14] *Annual Estimates of the Population of Metropolitan and Micropolitan Statistical Areas: April 1, 2000 to July 1, 2009 (CBSA-EST2009-01)*, U.S. Census Bureau, Population Division, Mar. 2010 [Online]. Available: http://www.census.gov/popest/data/metro/totals/2009/tables/CBSA-EST2009-01.xls.

[15] *The DARPA CORONET topology for the Contiguous United States (CONUS)* [Online]. Available: http://monarchna.com/CORONET_CONUS_Topology.xls.

Sheryl L. Woodward (M'91, SM'97) received her B.S. degree (*summa cum laude*) in physics and mathematics from the University of California, Los Angeles, in 1983 and her M.S. and Ph.D. degrees from the California Institute of Technology, Pasadena, in 1985 and 1988, respectively. Since then she has been a member of the Optical Systems Research Department at AT&T. Over the years she has done research on topics ranging from analog lightwave transmission for CATV to modulation formats for long-haul transmission. Her current research focuses on architectures and technologies relevant to optical backbone networks. She has authored or co-authored over 60 refereed journal and conference publications and holds 42 US patents.

Dr. Woodward is a member of the IEEE Photonics Society, and has served as Program and General Chair of the Annual Meeting (2006/2008). She recently was awarded the AT&T Science and Technology Medal for her work on network reliability.

Mark D. Feuer (M'87, SM'04) received his B.A. degree in physics from Harvard University, Cambridge, MA, and his Ph.D. degree in solid-state physics from Yale University, New Haven, CT. He is currently a Senior Scientist in Optical Systems Research at AT&T Labs, Middletown, NJ, focusing on enabling technologies for dynamic photonic networks. His current research interests include node architectures for wavelength routing, digital encoding methods for lightpath labels, and network optimization of space division multiplexing. In prior research at JDS Uniphase, AT&T Labs, and Bell Labs, he has studied optical metro networks, semiconductor and erbium-doped fiber amplifiers for access applications, electro-optic characterization of ultra-broadband transistors, and the physics and fabrication of compound semiconductor electronics. He has authored or co-authored over 120 refereed journal and conference publications and holds 24 US patents.

Dr. Feuer is a member of the IEEE Photonics Society and the American Physical Society (APS). He has served as General Chair of the Optical Fiber Communications Conference OFC/NFOEC2009 and is an Adjunct Professor of Electrical Engineering at Columbia University.

Inwoong Kim has been a member of the research staff in Fujitsu Laboratories of America since 2007. His research focuses on optical communications and networking.

He received his master's degree in physics from KAIST, the Korea Advanced Institute of Science and Technology, in 1993. He was a member of the Laser Application Group at the Korea Institute of Machinery and Materials from 1993 to 1998. He joined the Ultra-short Pulse Laser Lab, KAIST, as a Researcher in 1998.

He studied photonics and optical communications from 2000 to 2006 at CREOL, The College of Optics & Photonics, at the University of Central Florida, and received his Ph. D. degree in optical engineering in 2006. He has demonstrated ultra-fast all-optical clock recovery of 180 GHz using multi-section gain-coupled DFB lasers. He has also researched all-optical processes, based on a phase-sensitive amplifier, for carrier recovery and regeneration of phase-modulated optical signals. He worked on coherent optical communications as a postdoctoral fellow at CREOL. He was awarded an SPIE scholarship in 2005. He is a member of the IEEE Photonics Society.

Paparao Palacharla is a senior researcher in the network system innovation group at Fujitsu Laboratories of America. He received his B.Tech. degree from the Indian Institute of Technology, Kharagpur, and his Ph.D. degree in electrical and computer engineering from the University of Iowa. He has previously worked at the National Research Council, Nortel Networks, and Fujitsu Network Communications in the areas of optical signal processing, optical interconnects, and optical networking. His current research interests are dynamic optical networks and OTN networks and their applications. He has over 20 patents either pending or issued and has published over 30 papers in refereed conferences and journals. He has served as a technical program committee member for OFC/NFOEC, GLOBECOM, and other conferences.

Xi Wang received his B.S. degree in electronic engineering from Doshisha University, Japan, in 1998, and his M.E. and Ph.D. degrees in information and communication engineering from the University of Tokyo in 2000 and 2003, respectively. He joined Fujitsu Laboratories of America, Inc., in 2007. His current research interests include architecture design, control and management of next-generation ROADM networks, OTN networks, packet optical networks, and future photonic switching networks. Dr. Wang is a member of the IEEE Communications Society.